



# Theoretical analysis on the forced ignition of a quiescent mixture by repetitive heating pulse

Dehai Yu, Zheng Chen\*

*SKLTCS, CAPT, BIC-ESAT, Department of Mechanics and Engineering Science, College of Engineering, Peking University, Beijing 100871, China*

Received 31 December 2021; accepted 19 June 2022  
Available online xxx

## Abstract

Recently, forced ignition by nanosecond-repetitive-pulsed-discharge (NRPD) has received great attention since it can greatly promote ignition. However, there is no theoretical analysis on ignition induced by multiple heating pulses such as NRPD. Therefore, this work attempts to provide a theoretical interpretation on the ignition of a quiescent, flammable mixture by multiple discharges and to assess the effects of repetitive pulse on ignition characteristics. Based on fully transient formulation, analytical expressions describing ignition kernel propagation induced by multiple pulses are derived. The key parameters of multiple pulse heating, such as energy distribution among individual pulse, intermittent duration between neighboring pulse and total pulse numbers are appropriately incorporated, and their effects on ignition characteristics are assessed. It is found that because of memory effect, the flame kernel continues to propagate after switching off the external heating source. Sequentially introducing identical heating pulses at appropriate intermittent duration repetitively exploits the memory effect during ignition kernel development and thus extends propagating distance of the flame front. The repetitive pulse heating can promote ignition capability due to the flame revitalization effect, i.e., ignition reinforcement to the flame front thanks to additional thermal energy supplied by subsequent pulse. This is consistent with the synergistic effect of NRPD observed in previous experimental studies. In particular, as the pulse number increases, the minimum ignition energy decreases and approaches to an asymptotic value. In the limit of large pulse number, it is found that the integration of the implicit expressions describing the ignition kernel evolution does not depend on the pulse number explicitly. This substantiates the invariance of minimum ignition energy with heating pulse number. The present theory explains the effects of multiple discharges on ignition and provides insights on ignition enhancement.

© 2022 The Combustion Institute. Published by Elsevier Inc. All rights reserved.

**Keywords:** Ignition; Repetitive pulse; Minimum ignition energy; Flame propagation

## 1. Introduction

To meet the increasing demand in environmental protection, advanced combustion technologies need to be developed, such as burning exceedingly lean stratified fuel/air mixtures or mixtures diluted

\* Corresponding author.

E-mail address: [cz@pku.edu.cn](mailto:cz@pku.edu.cn) (Z. Chen).

by exhausted gas recirculation [1–3]. Under such conditions, reliable forced ignition is a challenge, and it greatly affects the overall performance of the combustion devices. Here forced ignition refers to the transition of the fuel/air mixture from a non-reactive to a reactive state by external energy deposition. An ignition kernel is first generated and then it evolves into a self-sustained propagating flame for successful forced ignition.

Spark discharge is widely used in combustion facilities since it provides controllable and reliable ignition. Recently, forced ignition by nanosecond-repetitive-pulsed-discharge (NRPD) has received great attention since it can greatly promote ignition [4–8]. During nanosecond discharge, the dominant part of the deposited energy is distributed to electric and vibrational excitation and dissociation of gas molecules, which facilitates the initial fuel oxidation, and in the meanwhile increases the overall temperature of the combustible mixture. Xu et al. [6] investigated the evolution of the ignition kernel induced by NRPD in a lean propane/air mixture. They found that the minimum ignition energy (MIE) can be reduced by increasing the nanosecond discharge frequency and total pulse number. Wang et al. [7] assessed the effects of discharge frequency, pulse number, and input energy per pulse of NRPD on ignition kernel development in a quiescent hydrogen/air mixture via transient numerical simulations. Ombrello and coworkers [4, 5, 9, 10] studied the forced ignition by NRPD in flowing mixtures. They identified three distinct regimes, i.e., fully coupled, partially coupled and decoupled between sequential pulses [5, 10]. Castela et al. showed that nanosecond discharges could produce vortical fluid motion with characteristic recirculation frequency that brings in the fresh gas to the gap between the electrodes [11]. Dumitrache et al. proposed a model interpreting the generation of these vortices and their dependence on multiple hydrodynamic parameters [12]. The fluid flow induced by nanosecond discharge was found to considerably affect the ignition characteristics and outcome [13, 14]. Shy and coworkers [15, 16] observed that coherence between frequency of NRPD and the recirculation frequency of turbulent flow of reactant induce synergistic effect on the flame kernel development, which can promote ignition. It can be understood that equality of characteristic times for flow and the repetitive pulse may lead to more efficient transportation of ignition energy to the ignition kernel front and thus facilitates ignition.

The above experimental and numerical studies indicate that repetitive/multiple energy deposition has strong impact on ignition kernel development and may considerably promote ignition. This motivates the present theoretical study on the forced ignition of a quiescent mixture by repetitive pulse heating.

Theoretical studies on ignition usually consider the development of ignition kernel triggered by

constant-power heating at the center [17–20]. Beyond the critical heating power, the ignition kernel can evolve into a self-sustained expanding flame. Based on quasi-steady assumption, He [17] and Chen et al. [18] derived a nonlinear velocity-curvature relation describing the evolution of the ignition kernel in a quiescent mixture without and with radiative heat loss, respectively. Chen et al. [19] found that the MIE tends to be linearly proportional to the cube of the critical flame radius, which is different from Zel'dovich flame ball radius for large Lewis number. In our recent work [20], we have developed a fully transient formulation which can describe the unsteady effects during the transition of initial flame kernel to ever-expanding spherical flame. It was found that the transient ignition energy deposition and ignition kernel evolution may considerably affect key ignition parameters, such as critical ignition radius and MIE [20]. Currently, theoretical analysis on ignition induced by multiple heating pulses is still not in place, which further motivates the present study.

The objectives of this work are to provide a theoretical analysis on the ignition of a flammable mixture by multiple discharges and to assess the effects of repetitive pulse on ignition. We modify the transient formulation in [20] by incorporating multiple pulses. An analytical expression describing the ignition kernel development is derived, based on which the forced ignition process induced by multiple pulses is analyzed in depth.

This paper is organized as follows. In Section 2, the mathematical model and expressions describing the flame kernel development subject to repetitive pulse are briefly presented. In Section 3, the flame revitalization effect by neighboring pulses on ignition is examined, and its dependence on key parameters of the ignition scheme is discussed. The concluding remarks are given in Section 4.

## 2. Formulation

We analyze the development of a flame kernel initiated by transient heating in a quiescent mixture. The classical thermal-diffusive model is used here and it is capable of interpreting the key features of forced ignition according to Champion et al. [21]. The formulation is analogous to that adopted in our previous study and all the non-dimensional units are identical in accordance [20].

An overall one-step exothermic reaction is adopted here, and its reaction rate follows the Arrhenius law. In the limit of large activation energy, the reaction zone is infinitely thin, and the reaction rate can be modeled by a delta function. The non-dimensional reaction rate is [22–24]

$$\omega = [\varepsilon_T + (1 - \varepsilon_T)T_f]^2 \exp \left\{ \frac{Z(T_f - 1)/2}{\varepsilon_T + (1 - \varepsilon_T)T_f} \right\} \quad (1)$$

where  $T_f$  is the non-dimensional flame temperature,  $\varepsilon_T = \tilde{T}_u / \tilde{T}_{ad}$  the expansion ratio,  $Z = (1 - \varepsilon_T) \tilde{T}_a / \tilde{T}_{ad}$  the Zel'dovich number,  $\tilde{T}_u$  the ambient temperature,  $\tilde{T}_{ad}$  the adiabatic flame temperature, and  $\tilde{T}_a$  the activation temperature. The flame front separates the unburnt and burnt regions, in both of which, the reaction term does not appear explicitly. Therefore, the non-dimensional governing equations for temperature  $T$  and mass fraction of the deficient reactant  $Y_u$  are [20]

$$\frac{\partial T_i}{\partial t} = \frac{1}{r^2} \frac{\partial}{\partial r} \left( r^2 \frac{\partial T_i}{\partial r} \right), \quad i = u, b \quad (2)$$

$$\frac{\partial Y_u}{\partial t} = \frac{1}{Le} \frac{1}{r^2} \frac{\partial}{\partial r} \left( r^2 \frac{\partial Y_u}{\partial r} \right) \quad (3)$$

where  $Le$  is the Lewis number, and subscripts  $u$  and  $b$  refer to the unburnt and burnt regime, respectively.

Across the infinitely thin reaction zone, the following jumping conditions hold [18]

$$\left( \frac{\partial T_b}{\partial r} \right)_{R^-} - \left( \frac{\partial T_u}{\partial r} \right)_{R^+} \quad (4)$$

$$\frac{1}{Le} \left( \frac{\partial Y_u}{\partial r} \right)_{R^+} = \left( \frac{\partial T_b}{\partial r} \right)_{R^-} - \left( \frac{\partial T_u}{\partial r} \right)_{R^+} \quad (5)$$

where  $R$  is the flame radius and the subscripts  $R^+$  and  $R^-$  indicate the derivatives evaluated at the unburnt and burnt sides of the flame front, respectively.

The initial and boundary conditions can be specified as follows: at  $t = 0$ ,  $T_b = T_b^0$ ,  $T_u = 0$ , and  $Y_u = 1$ ; at  $r = 0$ ,  $r^2(\partial T_b / \partial r) = -Q(t)$ ; at  $r = R(t)$ ,  $T_b = T_f(R)$ ; at  $r \rightarrow \infty$ ,  $T_u = 0$ ,  $Y_u = 1$ . Here  $Q(t)$  represents the ignition energy imposed at the center of induced ignition kernel. Repetitive pulse can be expressed in terms of Heaviside function, denoted by  $H$ , in the following form

$$Q(t) = Q_m \sum_{k=1}^{2n_p} (-1)^{k+1} H(t - t_k) \quad (6)$$

where  $Q_m$  is the heating power of an individual pulse, and  $n_p$  the total number of pulses, in which the  $k^{th}$  pulse is initiated at  $t = 2k - 1$  and ends at  $t = 2k + 1$ , ( $k = 1, 2, \dots, n_p$ ).

The transient variation of temperature and mass fraction on either side of the reaction front can be obtained by analytically solving the governing equations (2) and (3) subject to the initial and boundary conditions. Due to space limit, the detailed derivations are included in the Supplementary Material. Here we directly present the analytical expressions describing the variation of flame radius,  $R$ , and flame temperature,  $T_f$ , in the course of time, and their final forms are

$$T_f = \frac{\vartheta_3(\chi_{u,Y}) / F_{u,Y} Le + f_b T_b^0 + Q_m S_k(t) / F_{b,T} R}{f_b + \vartheta_3(\chi_{u,T}) / F_{u,T}} \quad (7)$$

$$\vartheta_3(\chi_Y) / Le F_{u,Y} R = \omega \quad (8)$$

which appear as implicit ordinary differential equations for  $R$  since  $U = dR/dt$ . The relevant factors are defined as follows

$$\chi_{u,j} = e^{-\pi^2 / F_{u,T}^2 R^2 L_j}, \quad j = T, Y \quad (9)$$

$$F_{u,j} = \int_1^\infty \frac{e^{-L_j R U (s^2 - 1)/2}}{s^2} ds, \quad j = T, Y \quad (10)$$

$$L_T = 1, \quad L_Y = Le \quad (11)$$

$$S_k(t) = \sum_{m=1}^k (-1)^{m+1} \vartheta_4(\chi_{b,T}^{t-t_m}) \quad (12)$$

$$\chi_{b,T} = e^{-\pi^2 / F_{b,T}^2 R^2} \quad (13)$$

$$F_{b,T} = \frac{\sqrt{\pi} \operatorname{erf}(\sqrt{RU/2})}{2\sqrt{RU/2} e^{-RU/2}} \quad (14)$$

$$f_b = \frac{1}{F_{b,T}} - 1 + \frac{RU}{3F_{b,T}} (1 - \chi_{b,T}^t) \quad (15)$$

and the Jacobi theta functions  $\vartheta_3$  and  $\vartheta_4$  are

$$\vartheta_3(x) = 1 + 2 \sum_{n=1}^\infty x^{n^2} \quad (16)$$

$$\vartheta_4(x) = 1 + 2 \sum_{n=1}^\infty (-1)^n x^{n^2} \quad (17)$$

The step profile of initial temperature implies infinitely large heat loss at the edge of ignition kernel, which cannot support the flame structure at  $t = 0$ . In the course of time, thermal conduction tends to smooth the temperature jump. Therefore, it needs an induction period,  $t_{ig}$ , subsequent to which the local heat loss is in balance with heat release from chemical reaction, thus giving birth to flame structure. At given ignition kernel radius  $R_0$  with  $U = 0$ , the onset flame temperature  $T_b^0 = T_f(t = t_{ig})$  in association with the induction time  $t_{ig}$  for the appearance of ignition kernel can be determined via the matching conditions, which exhibit in the following form

$$T_b^0 = \frac{1}{Le} \frac{\vartheta_3(\chi_{u,Y}^{t_{ig}})}{\vartheta_3(\chi_{u,T,0}^{t_{ig}})} + \frac{Q_m}{R_0} \frac{S_0(t_{ig})}{\vartheta_3(\chi_{u,T,0}^{t_{ig}})} \quad (18)$$

$$\frac{\vartheta_3(\chi_{u,Y}^{t_{ig}})}{Le R_0 F_{u,Y}} = \omega_0 \quad (19)$$

where  $\omega_0$  refers to the reaction rate by replacing  $T_f$  by  $T_b^0$  in Eq. (1), and the subscript "0" in remaining quantities, e.g.,  $\chi_{u,j}$  and  $S$ , indicates that those quantities are evaluated at the initial state of the

ignition kernel, i.e.  $R = R_0$  and  $U = 0$ . Our previous study [20] demonstrated that the value of  $R_0$  has negligible influence on the dynamic behavior of ignition kernel evolution, and thus the initial ignition kernel radius is selected to be  $R_0 = 0.01$  in this work.

Solving Eqs. (7) and (8) numerically gives the flame radius history,  $R(t)$ , and thereby determines the flame temperature,  $T_f(t)$  and flame propagation speed,  $U(t)$ . This transient formulation can describe forced ignition of combustible mixture induced by repetitive pulse, and it is used in the next section.

### 3. Results and discussion

According to previous studies [17, 20], the flame front continues to propagate outwardly for a while after removing the external heating source. Such phenomenon is known as memory effect and plays a crucial role in analyzing the dynamic behavior of flame kernel evolution as well as in determining the MIE, denoted by  $E_{min}$  [17, 20]. For ignition induced by repetitive pulse heating, the memory effect would become increasingly pronounced and can be investigated by means of the transient formulation presented in Section 2.

For typical premixed flames, we choose  $Z = 10$ , and  $\varepsilon_T = 0.15$  according to existing studies [19, 20, 22]. The effect of Lewis number on transient ignition process has been investigated in our previous study [20], and here we proceed the calculation in the following discussion by choosing  $Le = 2$ . A large Lewis number is chosen due to two reasons. First, the MIE increases with  $Le$  and it is difficult to achieve successful ignition for large  $Le$ . Second,

fuel-lean mixtures of large hydrocarbons used in engines have  $Le > 1$ . NRPD or multiple heating pulses can be used to promote ignition in mixtures with large  $Le$ .

The distribution of ignition energy among various heating pulses can be realized in multiple ways. In general, each heating pulse is characterized by heating duration, denoted by  $t_h^{(i)}$ , and intermittent duration,  $t_{im}^{(i)}$ . The period of individual pulse is  $t_p^{(i)} = t_h^{(i)} + t_{im}^{(i)}$ . Consequently, there will be  $2n_p$  degrees of freedom to completely define the external heating with  $n_p$  pulses, which becomes prohibitive to deal with analytically when  $n_p$  is large. We shall first consider the simplest case with double pulses.

#### 3.1. Double-pulse central heating

For even distribution of total ignition energy, denoted by  $E_{ig}$ , the heating duration for each pulse is  $t_h = E_{ig}/n_p Q_m$ . In terms of  $t_h$  and  $t_{im}$ , an intermittent factor is defined as  $\lambda_{im} = t_{im}/(t_h + t_{im})$ . Fig. 1 shows the temporal variation of propagation speed and flame temperature of flame front induced by single and double pulses. The total ignition energy is kept the same. It is seen that after switching off the first pulse, the ignition kernel expansion decelerates more severely in comparison with that driven by single pulse since only half of ignition energy is provided by the first pulse. When the second pulse is introduced, the flame kernel tends to be revitalized, as indicated by the inflexion points indicated by gray circle in Fig. 1. The flame revitalization can be understood that the second pulse provides fresh energy, which delays the flame temperature drop and thus boosts the

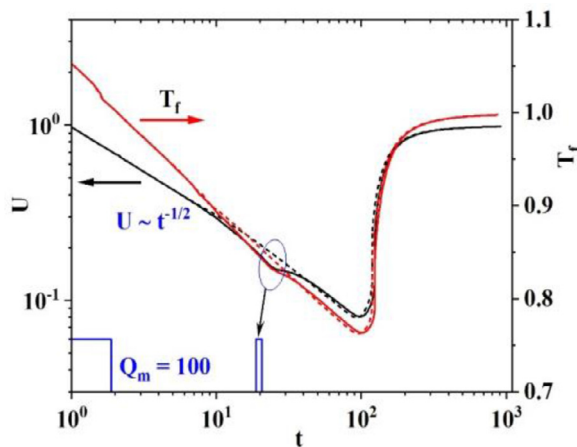


Fig. 1. The temporal variation of flame propagation speed (in black) and flame temperature (in red) as the ignition kernel evolves into a self-sustained expanding flame. The solid and dashed lines are for double and single pulse, respectively. Each heating scheme is characterized by identical ignition energy  $E_{ig} = 380$  and heating power  $Q_m = 100$ . The instants corresponding to the switching-on and -off of individual pulse are indicated by the squares adjacent to the abscissa for two pulse cases.

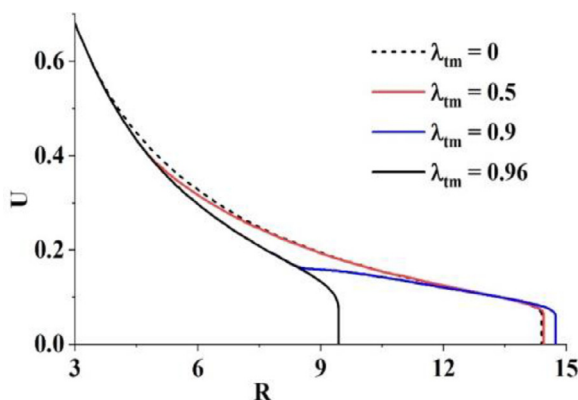


Fig. 2. The U-R diagram of flame kernel evolution with same subcritical ignition energy ( $E_{ig}=300$ ) and heating power ( $Q_m=100$ ) but deposited with different intermittent durations. Note that the MIE is  $E_{min}=365$ .

propagating speed of the flame front, compared to the cases of single pulse. As the ignition kernel evolves into the self-sustained expanding flame, the central heating has minor influence on subsequent propagation, and thereby the solid and dashed lines coincide.

The critical ignition state is determined by means of trial and error, and the MIE is calculated through Newton's bisection method when the gap shrinks below a threshold value, i.e.,  $\Delta E = 1$ . For  $E_{ig} < E_{min}$ , the flame front may propagate to a maximum distance, denoted by  $R_p$ , beyond which extinction occurs. The value of  $R_p$  increases with  $E_{ig}$  and can be used to measure the ignitability of the heating scheme. Fig. 2 shows that depositing ignition energy by double pluses may increase the propagating distance due to revitalization effect. The second pulse delivers ignition energy to the flame front, facilitating the chemical reaction there and resulting in a longer propagating distance. As  $\lambda_{tm}$  changes from 0.9 to 0.96, the propagating distance drops significantly. It is because the flame front undergoes extinction before receiving the revitalizing energy from the second pulse.

Given ignition energy, there exists a critical intermittent factor, denoted by  $\lambda_{tm,cr}$ , which corre-

sponds to the largest propagating distance. As heating power increases, the memory effect becomes stronger [20] and accordingly  $\lambda_{tm,cr}$  grows, as shown in Fig. 3.

Such phenomena could be understood as follows. The scaling relation  $U \sim t^{-1/2}$ , as indicated in Fig. 1(a), is consistent with  $R \sim t^{1/2}$  given by Buckmaster and Joulin [25], which implies that the product  $RU$ , denoted by  $\alpha_F$ , changes slowly with  $t$ . Moreover, according to numerical solutions, the magnitude of  $\alpha_F$  is approximately  $O(10)$ . The factors  $F_{u,T}$ ,  $F_{u,Y}$  and  $F_{b,T}$  can be asymptotically expressed in terms of  $\alpha_F$ , i.e.,  $F_{u,T} \sim 1/\alpha_F$ ,  $F_{u,Y} \sim 1/\alpha_F Le$ , and  $F_{b,T} \sim e^{\alpha_F/2}$ . Accordingly, the flame temperature would be simplified to

$$T_f \sim T_b^0 + Q_m e^{-\alpha_F/2} / \alpha_F R \quad (20)$$

It indicates that the flame temperature falls during expansion. There exists a critical flame temperature, denoted by  $T_{cr}$ , below which chemical reaction cannot sustain the flame structure, and consequently the revitalizing effect of subsequent pulse turns to be futile. As heating power increases, the relatively more rapid deposition of ignition energy leaves less time for heat loss at the flame front, and thus the flame structure at the ignition kernel edge

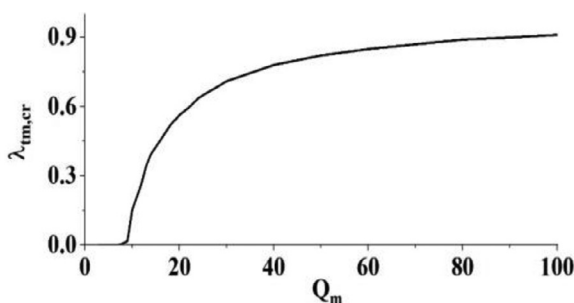


Fig. 3. Change of critical intermittent factor  $\lambda_{tm,cr}$  with heating power  $Q_m$ . The ignition energy is fixed as  $E_{ig} = 300$ .



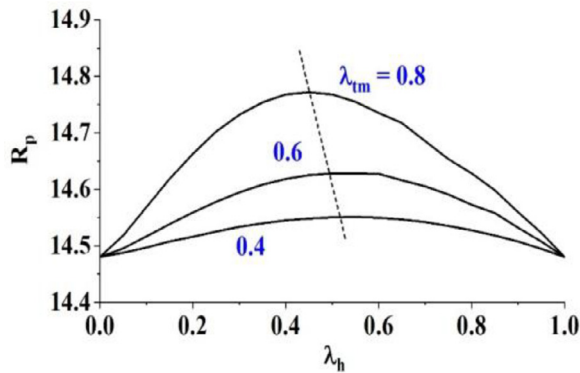


Fig. 4. The variation of propagating distance with uneven distribution of ignition energy to each pulse. The heating scheme is identical to that in Fig. 2.

could sustain more distantly from the heating center. It provides longer time for the second pulse to transfer fresh thermal energy to the flame front i.e., the intermittent duration between pulses can be made larger. Accordingly, the critical intermittent factor grows with heating power.

In the preceding discussion, each heating pulse delivers the same amount of energy. In general, the ignition energy can be arbitrarily distributed between each second pulse. Denoting the heating duration for the first and the second pulses by  $t_{h1}$  and  $t_{h2}$ , we define the heating factor as  $\lambda_h = t_{h1}/(t_{h1} + t_{h2})$ , which characterizes the ratio of the energy deposition by the first pulse to the total ignition energy. The uneven distribution of ignition energy can change the propagating distance of the flame front, as indicated in Fig. 4. In both limits of  $\lambda_h \rightarrow 0$  and  $\lambda_h \rightarrow 1$ , the heating scheme is reduced to single pulse, which leads to relatively shorter propagating distance.

The non-monotonic change of  $R_p$  with  $\lambda_h$  shown in Fig. 4 suggests the existence of optimal heating factor,  $\lambda_{h,cr}$ , which leads to the largest propagating distance. Fig. 4 shows that the  $\lambda_{h,cr}$  takes the intermediate value and slightly decrease as extending the intermittent duration. For small  $\lambda_h$ , the flame front could move to some distance from the center, despite of the relatively low energy deposition. While the flame temperature given by Eq. (20) implies that the impact of central heating becomes less effective as flame front propagating outwardly. Therefore, significant amount of ignition energy devoted by the second pulse may not be efficiently utilized to drive the propagation of flame front. In the opposite limit of large  $\lambda_h$ , the second pulse, containing small amount of ignition energy, may have little contribution to affect the flame front resulting from the first pulse at large distance. It is hypothesized that each pulse would have comparable capability to sustain the flame kernel expansion when ignition energy is evenly distributed, thus corresponding to the longest propagating distance. In

the following discussion, we shall consider forced ignition cases with even distribution of ignition energy among individual pulse.

Preceding discussion demonstrates the facilitating effect of double pulse heating on the forced ignition process. The dashed line in Fig. 5(a) shows that for slightly subcritical ignition energy,  $E_{ig} = 350$ , heating by single pulse leads to  $R_p \approx 17$ , beyond which the flame front undergoes extinction. Moderately increasing the intermittent factor to  $\lambda_{im} = 0.6$ , the propagating distance becomes slightly longer. However, flame extinction still occurs. Tuning the intermittent factor close to the critical value,  $\lambda_{im} = 0.93$ , the flame front can successfully move across the critical radius, and subsequently a self-sustained expanding flame is established and continues to propagate outwardly. The U-R diagram for  $\lambda_{im} = 0.93$  in Fig. 5(a) indicates that noticeable flame revitalization induced by the second pulse occurs around  $R = 10$ , which helps to achieve successful ignition.

Before arriving at the critical radius, the temperature at the flame front falls as the ignition kernel expands because the heat loss through thermal conduction exceeds heat release from chemical reaction. Subsequent to the removal of external heating pulse, the average temperature inside the ignition kernel decreases. Fig. 5(b) compares the evolution of the temperature profiles corresponding to single pulse (dashed line) and double pulses (solid lines) across the flame front. Close to the heating center, e.g.,  $R = 3$ , the temperature profile inside the flame kernel is downwardly convex, indicating that thermal energy is acceleratingly transferred towards the flame front in the presence of central heating. After ignition energy deposition, the central temperature drops exceedingly rapidly, and the temperature profile continuously evolves into an upwardly convex type, implying that energy is deceleratingly supplied to the flame front.

Interestingly, at the distance of  $R = 10$ , the flame temperature profile in the burnt region correspond-

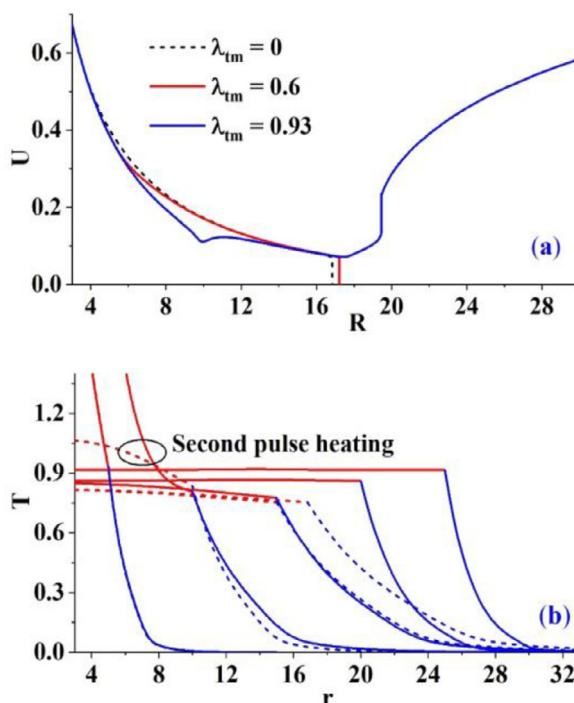


Fig. 5. (a) The impact of two-pulse heating on ignitability, in which the same amount of ignition energy  $E_{ig} = 350$  is released at constant heating power  $Q_m = 100$  with various intermittent durations; (b) The comparison of temperature profiles at selected instants (or equivalently the flame front locations) characterizing the flame kernel evolution corresponding to conditions of  $\lambda_{tm} = 0$  (dashed lines) and  $\lambda_{tm} = 0.93$  (solid lines).

ing to double pulse ( $\lambda_{tm} = 0.93$ ) remains to be downwardly convex though the local flame temperature is lower than that for single pulse ( $\lambda_{tm} = 0$ ). It can be understood as follows. When the second pulse is imposed, the central temperature grows exceedingly high due to the zero-dimension of the external heating source. Consequently, the substantial transient thermal conduction to the ignition kernel front takes place, which is manifested by the downwardly convex temperature profiles as captured by the last two time instants of the solid lines.

The change in the geometry of temperature profiles inside the flame kernel clearly unveils the mechanism of flame revitalization. The second pulse provides an additional amount of energy to flame front to assist its propagation. It helps the ignition kernel cross the critical radius ( $R_{cr} \approx 19$  for  $Le = 2.0$ ) and eventually become a self-sustained flame. The transition from non-successful to successful ignition as increasing the intermittent factor from  $\lambda_{tm} = 0$  to  $\lambda_{tm} = 0.93$  proves that changing from the single pulse to double pulses central heating can reduce the MIE and thus promote ignition.

The revitalization effect, exhibited in Fig. 5, interprets the mechanism of ignition enhancement by NRPD from the aspect of ignition reinforcement between sequential pulses [15, 16]. In turbu-

lent flows, the recirculating eddies generate possibility that the ignition energy deposited by repetitive pulses can be more readily transported to the flame front. The convective heat transfer could be much more effective than pure conduction and thus may lead to considerable acceleration of the revitalization process, which is consistent with the synergistic effect of NRPD [15, 16].

### 3.2. Multi-stage central heating

The controlling factors that affect the performance of multi-stage heating are the thermal energy per pulse  $E_{imp}$ , total pulse number  $n_p$ , and intermittent factor  $\lambda_{tm} = t_{im}/(t_h + t_{im})$  for individual pulse. The effects of these factors on the critical ignition condition and ignition kernel propagation are assessed, and typical results are depicted in Fig. 6.

Fig. 6(a) shows that sequentially adding pulses promotes the propagating distances with identical intermittency factor  $\lambda_{tm} = 0.9$ . In each heating scheme, the first pulse generates a comparably longer propagating distance since the ignition energy can be more readily transferred to the flame front. Interestingly, the increments of  $R_p$  tends to be linearly proportional to  $n_p$  for  $n_p \geq 2$ , which may be understood as follows. The increasing distance

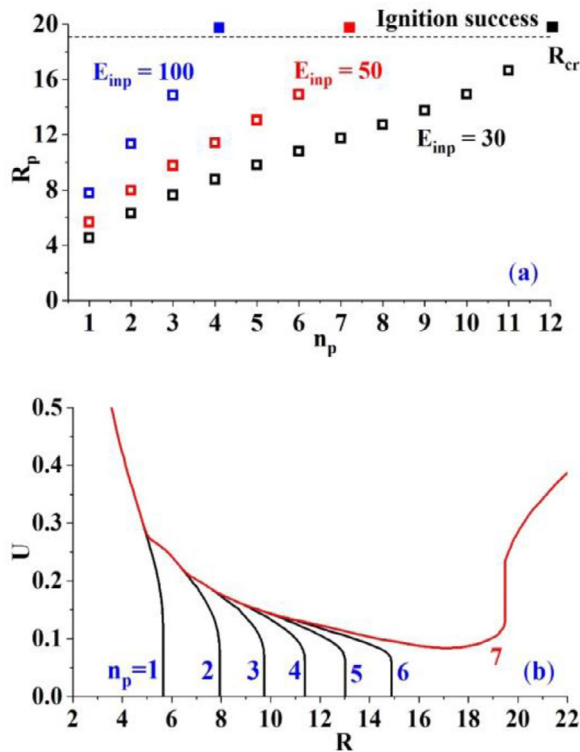


Fig. 6. (a) Change of propagating distances (hollow symbols) with the pulse numbers. The critical radius is represented by the dashed line, above which the solid symbols denote successful flame initiation. (b) The U-R diagrams characterizing the dynamic behavior of flame front propagation by sequentially adding each pulse with identical ignition energy  $E_{imp} = 50$  at identical heating power  $Q_m = 100$  and intermittent factor  $\lambda_{im} = 0.9$ .

of the flame front from the heating center lowers the ignition capability of the subsequent pulses according to Eq. (20) and thus tends to shorten the propagating distances. In the meanwhile, the inhibiting effect of positive curvature on flame propagation in mixture with  $Le > 1$  is alleviated at large distance. It is noted that the distance between  $R_{cr}$  (dashed line in Fig. 6a) and  $R_p$  corresponding to the final pulse, which leads to flame initiation (the highest hollow symbols in Fig. 6a), appears to be slightly larger than the historical increment of  $R_p$  led by each previous pulses for  $n_p \geq 2$ . It can be understood as follows. As  $R \rightarrow R_{cr}$ , the rate of preheating unburnt mixture, characterized by the flame front curvature,  $\kappa \sim 1/R$ , approaches to the rate of heat generation by chemical reaction. The flame temperature tends to change slowly due to such nearly balanced budget in heat transfer across the flame front. Therefore, the facilitating efficiency of the final pulse is promoted, which then leads to larger increment of propagating distance.

The turning points on the solid lines in Fig. 6(b) indicate successive flame revitalization led by adding individual pulse. Besides, it shows that near the critical radius, the propagation speed of flame front tends to remain constant instead of contin-

uously decreasing at shorter distances. It is consistent with the slowly variation of flame temperature due to the near equilibrium heat flux across the flame front.

By means of multiple pulses, the forced ignition can be made more flexible. In addition to intermittent factors, the ignition is also affected by the total pulse number  $n_p$ . Fig. 7 shows the effects of pulse number and intermittent factor on the propagating distance of flame kernel driven by a single and multiple pulses with the same amount of ignition energy. Fig. 7 indicates that distributing ignition energy into more pulses leads to longer propagating distance. This is because the flame front experiences sequential revitalization, which takes more advantage of the memory effect of central heating. However, such additional increment of  $R_p$  appears to be indiscernible as increasing  $n_p$ , we may hypothesize that the ignition behavior would be independent of the pulse number in the limit of  $n_p \rightarrow \infty$ .

Fig. 7 shows that at each pulse number, the propagating distance changes nonmonotonically with intermittent factor. For  $\lambda_{im} > 0.95$ , the  $R_p$ - $\lambda_{im}$  curves undergo sudden drop and then turns into platform. It implies that extinction occurs after the first pulse expires and that the second pulse is



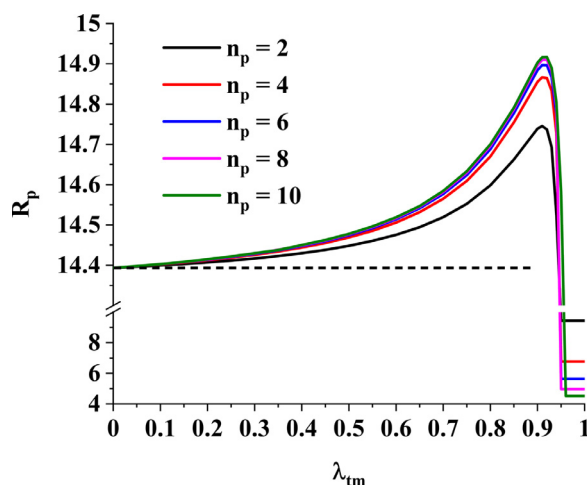


Fig. 7. Change of propagating distance with intermittent factor for flame kernel propagation driven by multiple heating pulses with fixed ignition energy of  $E_{ig} = 300$  and heating power of  $Q_m = 100$ . The dashed line represents the results for single pulse.

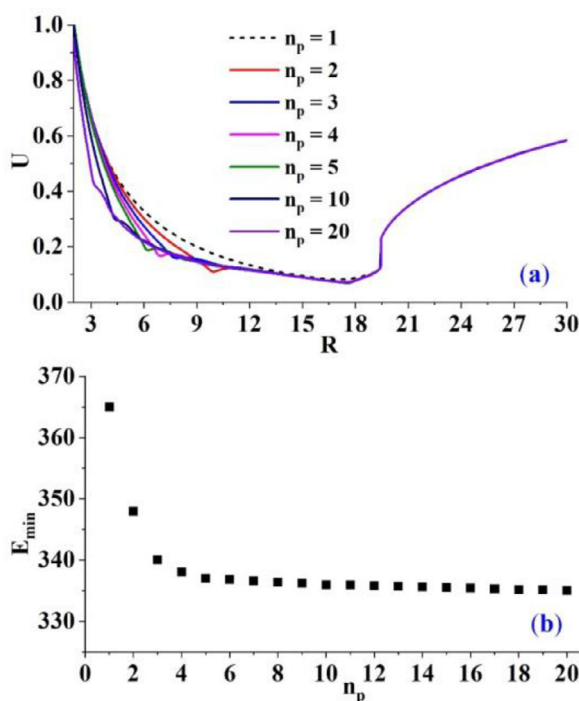


Fig. 8. (a) The dynamic behavior of flame kernel development induced by multiple pulses external heating with identical power  $Q_m = 100$ . At each pulse number, the energy deposition is equal to the corresponding MIE with  $\lambda_{tm} = 0.9$ . (b) The variation of minimum ignition energies with pulse number.

unable to reignite the flame in such long intermittent duration. Most importantly, Fig. 7 shows that the critical intermittent duration is around 0.9, which is consistent with the results shown in Fig. 3 for cases with double pulse.

Increasing pulse number affects the history of flame kernel development during its transition to self-sustained spherical flame. Therefore, the MIE depends on  $n_p$  as shown in Fig. 8. Each curve in Fig. 8(a) represents the U-R diagram of flame front

driven by ignition energy equal to MIE. As  $n_p$  increases, the U-R curve becomes wrinkled at multiple points, which demonstrates flame revitalization by the subsequent heating pulse. Generally, the U-R curve falls as  $n_p$  increasing and approximately approaches toward a limiting envelope at sufficiently large  $n_p$ . Fig. 8(b) shows that the MIE gradually decays with pulse numbers. In the limit of  $n_p \rightarrow \infty$ , the heating duration for individual pulse is so short that the thermal energy addition can be considered being instantaneous. Therefore, the heating scheme can be written as

$$Q(t) = \sum_{k=1}^{n_p} \frac{E_{ig}}{n_p} \delta(t - \tau_k) \quad (21)$$

which implies that the heating power for individual pulse would be infinitely high. Substituting Eq. (21) into the matching conditions (7) and (8) and integrating with respect to time, it involves a summation of quantities at selected instants  $\tau_k$ . It can be shown that those quantities hardly depend on  $n_p$ . Consequently, the pulse number on the denominator approximately cancels out with the summation. Since the pulse number would not appear explicitly in the final solutions for the location and temperature of the flame front, it suggests the independence of MIE upon  $n_p$  in the limit of  $n_p \rightarrow \infty$ .

#### 4. Concluding remarks

A fully transient formulation is proposed to analyze the development of an ignition kernel in a quiescent mixture subject to multiple pulses of central heating. First, we derive a pair of implicit ordinary differential equations, which can describe the transient evolution of the ignition kernel induced by multiple pulses. Then, the effects of energy distribution among each pulse, the intermittent duration between neighboring pulses, and the total pulse number on flame kernel evolution are assessed.

It is found that splitting continuous external heating into multiple pulses with equal distribution of thermal energy leads to longer propagating distance of the flame front of the ignition kernel. Therefore, consistent with previous ignition experiment using NRPD, repetitive pulse central heating can promote ignition by recurrently exploiting memory effect of flame front propagation. This exhibits the mechanism of flame revitalization, i.e., the sequential pulses constantly provide ignition energy reinforcement to prompt the ignition kernel expansion. The MIE decreases towards an asymptotic value at sufficiently large pulse number. When the pulse number are sufficiently large, the heating duration of individual pulse becomes exceedingly short, which can be regarded as instantaneous release of ignition energy. Accordingly, the pulse number would not appear explicitly in the solutions

of the implicit ODEs describing the ignition kernel evolution, which substantiates the constancy of MIE at large pulse numbers.

It is noted that a quiescent mixture is considered in the present theory. In actual ignition process, the mixture might not be static. Nevertheless, the analytical solution cannot be obtained when the discharge-induced fluid motion is incorporated in the present formulation. In addition, for real fuels with finite reaction layer thickness, the reaction rate would be lower than that given by Eq. (1). Accordingly, the revitalization effect may become less profound since the response of flame front to heating pulse may become less sensitive. Nevertheless, the forced ignition by NRPD is an exceedingly complex process in real-life situations. Both thermal and chemical effects, characterized by temperature increase in ignition kernel and generation of key radicals respectively, contribute to ignition. Therefore, it is difficult to include all factors in theoretical analysis on the dynamic behavior of ignition kernel development. In future works, it would be interesting to conduct numerical simulations to assess the effects of fluid motion on forced ignition by repetitive pulse heating, which is close to experiments and meets practical concern.

#### Declaration of Competing Interest

The authors declare that they have no known competing financial interests or personal relationships that could have appeared to influence the work reported in this paper.

#### Acknowledgements

This work was supported by [National Natural Science Foundation of China](#) (nos. 52006001 and 52176096). We thank helpful discussion with Dr. Xinyi Chen and Mr. Shumeng Xie at Peking University.

#### Supplementary materials

Supplementary material associated with this article can be found, in the online version, at doi:[10.1016/j.proci.2022.06.014](https://doi.org/10.1016/j.proci.2022.06.014).

#### References

- [1] N. Hayashi, A. Sugiura, Y. Abe, K. Suzuki, Development of ignition technology for dilute combustion engines, *SAE Int. J. Engines* 10 (2017) 984–994.
- [2] S. Tsuboi, S. Miyokawa, M. Matsuda, T. Yokomori, N. Iida, Influence of spark discharge characteristics on ignition and combustion process and the lean operation limit in a spark ignition engine, *Appl. Energy* 250 (2019) 617–632.

- [3] S. Yu, M. Zheng, Future gasoline engine ignition: A review on advanced concepts, *Int. J. Engine Res.* 22 (2021) 1743–1775.
- [4] K.C. Opacich, T.M. Ombrello, J.S. Heyne, J.K. Lefkowitz, R.J. Leiweke, K. Busby, Analyzing the ignition differences between conventional spark discharges and nanosecond-pulsed high-frequency discharges, *Proc. Combust. Inst.* (2021).
- [5] N.R. Tichenor, R.J. Leiweke, T.M. Ombrello, in: *Effects of Fuel Mixture Properties on Nanosecond Pulsed High Frequency Discharge Ignition*, 2019, p. 0461. AIAA Scitech 2019 Forum.
- [6] D. Xu, D. Lacoste, C. Laux, Ignition of quiescent lean propane–air mixtures at high pressure by nanosecond repetitively pulsed discharges, *Plasma Chem. Plasma Process.* 36 (2016) 309–327.
- [7] Y. Wang, P. Guo, H. Chen, Z. Chen, Numerical modeling of ignition enhancement by repetitive nanosecond discharge in a hydrogen/air mixture II: forced ignition, *J. Phys. D* 54 (2020) 065502.
- [8] Y. Ju, W. Sun, Plasma assisted combustion: Dynamics and chemistry, *Prog. Energy Combust. Sci.* 48 (2015) 21–83.
- [9] W. Sun, S.H. Won, T.M. Ombrello, C. Carter, Y. Ju, Direct ignition and S-curve transition by in situ nano-second pulsed discharge in methane/oxygen/helium counterflow flame, *Proc. Combust. Inst.* 34 (2013) 847–855.
- [10] J.K. Lefkowitz, T.M. Ombrello, An exploration of inter-pulse coupling in nanosecond pulsed high frequency discharge ignition, *Combust. Flame* 180 (2017) 136–147.
- [11] M. Castela, S. Stepanyan, B. Fiorina, A. Coussement, O. Gicquel, N. Darabiha, C.O. Laux, A 3-D DNS and experimental study of the effect of the recirculating flow pattern inside a reactive kernel produced by nanosecond plasma discharges in a methane-air mixture, *Proc. Combust. Inst.* 36 (2017) 4095–4103.
- [12] C. Dumitrache, A. Gallant, N. Minesi, S. Stepanyan, G.D. Stancu, C.O. Laux, Hydrodynamic regimes induced by nanosecond pulsed discharges in air: mechanism of vorticity generation, *J. Phys. D* 52 (2019) 364001.
- [13] S. Lovascio, T.M. Ombrello, J. Hayashi, S. Stepanyan, D. Xu, G.D. Stancu, C.O. Laux, Effects of pulsation frequency and energy deposition on ignition using nanosecond repetitively pulsed discharges, *Proc. Combust. Inst.* 36 (2017) 4079–4086.
- [14] S. Stepanyan, N. Minesi, A. Tibère-Inglesse, A. Salmon, G.D. Stancu, C. Laux, Spatial evolution of the plasma kernel produced by nanosecond discharges in air, *J. Phys. D* 52 (2019) 295203.
- [15] S.S. Shy, Y.R. Chen, B.-L. Lin, A. Maznoy, Ignition enhancement and deterioration by nanosecond repetitively pulsed discharges in a randomly-stirred lean n-butane/air mixture at various inter-electrode gaps, *Combust. Flame* 231 (2021) 111506.
- [16] M. Nguyen, S. Shy, Y. Chen, B. Lin, S. Huang, C. Liu, Conventional spark versus nanosecond repetitively pulsed discharge for a turbulence facilitated ignition phenomenon, *Proc. Combust. Inst.* 38 (2021) 2801–2808.
- [17] L. He, Critical conditions for spherical flame initiation in mixtures with high Lewis numbers, *Combust. Theory Model* 4 (2000) 159–172.
- [18] Z. Chen, Y. Ju, Theoretical analysis of the evolution from ignition kernel to flame ball and planar flame, *Combust. Theory Model* 11 (2007) 427–453.
- [19] Z. Chen, M.P. Burke, Y. Ju, On the critical flame radius and minimum ignition energy for spherical flame initiation, *Proc. Combust. Inst.* 33 (2011) 1219–1226.
- [20] D. Yu, Z. Chen, Theoretical analysis on the transient ignition of premixed expanding flame in a quiescent mixture, *J. Fluid Mech.* 924 (2021).
- [21] M. Champion, B. Deshaies, G. Joulin, Relative influences of convective and diffusive transports during spherical flame initiation, *Combust. Flame* 74 (1988) 161–170.
- [22] Y.C. Wu, Z. Chen, Asymptotic analysis of outwardly propagating spherical flames, *Acta Mech. Sin.* 28 (2012) 359–366.
- [23] C.K. Law, *Combustion Physics*, Cambridge University Press, 2006.
- [24] A. Veeraragavan, C.P. Cadou, Flame speed predictions in planar micro/mesoscale combustors with conjugate heat transfer, *Combust. Flame* 158 (2011) 2178–2187.
- [25] J. Buckmaster, G. Joulin, Radial propagation of premixed flames and t behavior, *Combust. Flame* 78 (1989) 275–286.